Physics in Medicine &
Biology

PAPER • **OPEN ACCESS**

Impact of manufacturing tolerances on Monte Carlo calculated k_{Q,Q_0} factors for plane-parallel ionisation chambers in proton beams

To cite this article: Guillaume Houyoux *et al* 2025 *Phys. Med. Biol.* **70** 085012

IOP Publishing Phys. Med. Biol. 70 (2025) 085012 https://doi.org/10.1088/1361-6560/adc86b

Physics in Medicine & Biology

IPEM Institute of Physics and Engineering in Medicine

OPEN ACCESS

RECEIVED
5 November 2024

REVISED
11 February 2025

ACCEPTED FOR PUBLICATION
2 April 2025

PUBLISHED
15 April 2025

PAPER

Impact of manufacturing tolerances on Monte Carlo calculated k_{Q,Q_0} factors for plane-parallel ionisation chambers in proton beams

Guillaume Houyoux[1,*], Sébastien Penninckx[1,2], Séverine Rossomme[3], Kevin Souris[3], Hugo Palmans[4,5] and Nick Reynaert[1]

[1] Radiophysics and MRI Physics Laboratory, Faculty of Medicine, Université Libre de Bruxelles, Brussels, Belgium
[2] Department of Radiation Oncology, Institut Jules Bordet, Hôpital Universitaire de Bruxelles (HUB), Université Libre de Bruxelles, Brussels, Belgium
[3] Dosimetry Business Unit, Clinical, Ion Beam Applications, Louvain-La-Neuve, Belgium
[4] Medical Physics, MedAustron Ion Therapy Center, Wiener Neustadt, Austria
[5] Radiotherapy and Radiation Dosimetry, National Physical Laboratory, Teddington, United Kingdom
[*] Author to whom any correspondence should be addressed.

E-mail: Guillaume.Houyoux@ulb.be

Keywords: proton dosimetry, beam quality correction factor, manufacturing tolerances, TRS-398 CoP, Monte Carlo, GATE, Geant4

Supplementary material for this article is available online

Abstract

Objective. In the recent update of the TRS-398 Code of Practice (CoP), Monte Carlo results were incorporated into the derivation of recommended beam quality correction factors for ionisation chambers (IC) in proton beams. While the underlying Monte Carlo simulations implement detailed models only based on the nominal geometries from manufacturer blueprints, this paper considers the potential geometric deviations in plane-parallel IC arising from manufacturing tolerances that can reach 10%. *Approach.* A representative model of a plane-parallel IC has been designed using the Monte Carlo code GATE/Geant4, from which beam quality correction factors have been derived. Subsequently, the results of a reference geometry are compared to those of perturbed geometries, in which the parameters are modified according to the tolerances specified in a standard. *Main results.* The comparison between the reference and perturbed geometries reveals no significant differences, as they show an agreement within one standard deviation for all the cases studied, with relative deviations not exceeding 0.5%. From these results, we estimate the maximum added uncertainty from manufacturing tolerances on Monte Carlo calculated k_Q factors to be about 0.7%. *Significance.* Overall, the current use of nominal dimensions of plane-parallel IC from manufacturer's blueprints remains consistent for beam quality correction factor calculations via Monte Carlo simulations, which therefore support the latest results recommended by the TRS-398 CoP.

1. Introduction

The IAEA TRS-398 (2024) code of practice (CoP) provides recommended values for the beam quality correction factors, called k_{Q,Q_0} factors, that are currently required for air-filled ionisation chambers (IC) when calculating the absorbed dose to water in reference dosimetry. As the name suggests, this factor allows to take into account the differences between the user beam quality at the particle beam facility and the reference beam quality used in standard laboratories for absorbed dose to water calibration. In the recent update of the TRS-398 CoP, Monte Carlo (MC) calculated data for proton beams have been added to the experimental data obtained from calorimetry in order to derive the best estimates of k_{Q,Q_0} factors (Palmans *et al* 2022), resulting in a reduction in the overall uncertainty associated to k_{Q,Q_0} factors.

The MC results added in the TRS-398 CoP were evaluated by Baumann *et al* (2023), where the authors showed that the standard deviation of the MC calculated k_{Q,Q_0} values averaged over different MC codes

(between 0.7% and 1.2% depending on the beam energy) was well within the overall uncertainty estimated of 1.4% in the TRS-398 CoP, as individual IC characteristics can be accounted for with the MC. Indeed, although the current use of MC in the determination of k_{Q,Q_0} values is based on the calculation of dose deposition within the sensitive volume of an IC, which does not (yet) take into account the electronics of the detector nor the charge collection per se within the chamber, it still benefits from the detailed level of modelling that can be achieved from manufacturing blueprints. In this same study, (Baumann *et al* 2023) highlighted small differences in IC modelling from one publication to another. In general, the geometric differences were found either in the entrance window thickness of the IC where the deviations were smaller than 1%, or either in the collecting electrode thickness where the deviations could reach about 20% on submillimetric scales. However, the authors concluded that the effect on the overall uncertainty could be considered rather small compared to the larger influence of the transport parameters in MC codes.

In practice, geometric deviations between two ICs of the same model always occur. They are due to the manufacturing tolerances that are applied to the various parts constituting the IC, and they determine the dimensional range within which the size of the part is to be expected. These are defined as geometric margins within which the enablement of assembling the final product and its proper functioning are guaranteed. The most common way of defining these tolerances is through the DIN ISO 2768 (1989) standards, which classify them from fine to very coarse. These standards are intended to simplify technical drawings and specify general tolerances for linear and angular dimensions, shape and position without explicitly stating the tolerances themselves. Considering the typical size of IC parts between 1 mm and 10 mm, the finest ISO tolerances lead to an uncertainty that can reach about 10% in some cases. However, these tolerances are never taken into account when simulating ICs under proton beams with MC; instead, the ICs are always modelled with their nominal dimensions as provided by manufacturers. This problem has already been investigated for MeV photon beams in cylindrical ICs by Wulff *et al* (2010) and Muir and Rogers (2010), and in plane-parallel ICs by Muir *et al* (2012). For electron beams, the case of plane-parallel ICs was treated by Zink and Wulff (2012), and for cylindrical ICs by Muir and Rogers (2013). Nevertheless the question remains open for proton beams, and we can wonder whether or not this could affect the overall uncertainty of the MC calculated k_{Q,Q_0} factors compared to combined experimental data, which intrinsically account for these geometric variations by combining measurements from different physical detectors.

The aim of this study is to evaluate the sensitivity of MC calculated k_{Q,Q_0} factors for plane-parallel ICs under geometric perturbations coming from manufacturing tolerances. In this way, we aim to determine whether current MC results tend to underestimate their associated statistical uncertainty by considering fixed nominal IC geometries.

2. Materials and methods

The general method presented in this section is based on the work of Baumann *et al* (2020), where beam quality correction factors were calculated via MC for multiple ICs using TOPAS (Perl *et al* 2012).

2.1. Beam quality correction factor

The beam quality correction factors k_{Q,Q_0} were calculated according to Andreo *et al* (2013) as,

$$k_{Q,Q_0} = \frac{f_Q}{f_{Q_0}} \frac{W_{\text{air},Q}}{W_{\text{air},Q_0}} = \frac{(D_w/\bar{D}_{\text{air}})_Q}{(D_w/\bar{D}_{\text{air}})_{Q_0}} \frac{W_{\text{air},Q}}{W_{\text{air},Q_0}} \quad , \tag{1}$$

where the subscripts Q and Q_0 denote the user beam quality and the reference beam quality respectively. The quality-dependent and chamber-specific f factors (Sempau *et al* 2004) determine the proportionality between the absorbed dose to water at a point in the absence of the detector (D_w) and the averaged absorbed dose to air in the sensitive volume of the IC ($\bar{D}_{\text{air}}$). In this work, only the absorbed doses were calculated using MC while the mean energies required to create an ion in air (W_{air}) were taken from ICRU 90 (Seltzer *et al* 2016). In the following, the beam quality correction factor is referred to as k_Q, as it is conventionally used when the reference beam quality Q_0 is ^{60}Co gamma radiation (IAEA TRS-398 2024).

2.2. Geometries and materials

A simplified model of plane-parallel IC was considered, where the air cavity is embedded in a homogeneous cylinder of PEEK, an interesting material for ICs due to its radiation hardness (Kurtz 2012). The model, depicted in figure 1, was defined by five geometric parameters : the height and the radius of the air cavity, the thickness of the entrance and exit windows, and the lateral thickness of the body. A reference geometry was defined according to the averaged dimensions of plane-parallel ICs modelled in Gomà and Sterpin (2019) and in Baumann *et al* (2020). The reference values of each parameter are presented in table 1.

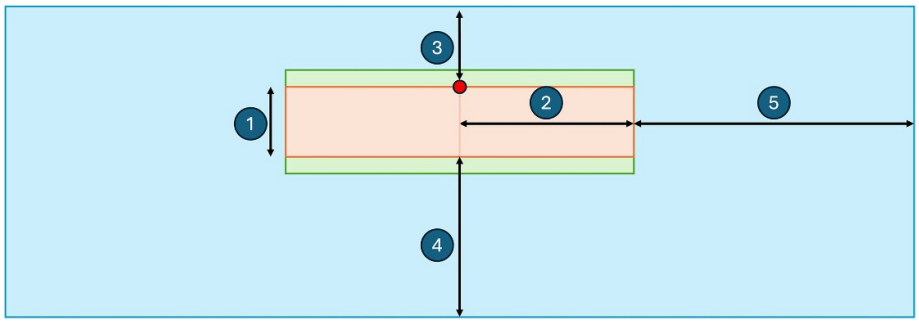

Figure 1. Cross-section of the representative model of a plane-parallel IC defined in this work. The body of the chamber is shown in blue, while the air cavity is represented in orange and the electrodes in green. Five geometric parameters define the model : (1) the height of the cavity, (2) the radius of the cavity, (3) the entrance window, (4) the exit window and (5) the lateral thickness of the body. The red dot indicates the reference point of measurement of the IC. For clarity, the model is not depicted with the right scale.

Table 1. Dimensions of reference and ISO tolerances applied on each parameter of the model.

Parameter	Reference (mm)	ISO tolerance (mm)
Cavity height	1.5	0.1
Cavity radius	5.0	0.5
Entrance window	1.0	0.1
Exit window	10.0	0.2
Lateral thickness	10.0	1.0

In order to study the influence of manufacturing tolerances on our model, the parameters were perturbed according to DIN ISO 2768 (1989) standards summarised in table 1 in accordance with the typical tolerances specified by ICs manufacturers. The medium class of tolerances *(m)* was applied both on the linear dimensions (cavity height, entrance window and exit window) and on the external radius dimensions (cavity radius and lateral thickness of the body), corresponding to perturbations between 2% and 10%.

2.2.1. Graphite electrodes

The electrodes composing plane-parallel ICs are typically made of a thin (submillimetric) coating of graphite, the thickness of which is hardly measurable and requires micro CT images (McNiven *et al* 2008). Assuming that small changes of the thickness could affect the energy deposited inside the air cavity, its effect was investigated by adding a first graphite layer inside the inner surface of the entrance window (top electrode) and a second layer within the inner surface of the exit window (collecting electrode). Following the representation of the model depicted in figure 1, the electrodes were placed inside the chamber body, keeping the total height of the IC constant and the size of the air cavity unaffected. In this work, the default thickness of the electrodes was considered to be 50 μm and we studied the k_Q sensitivity up to 100 μm.

2.2.2. PPC-like IC

From the reference geometry defined above, two particular cases closer to realistic plane-parallel ICs were selected to be studied in order to test the broad applicability of our model. The choice went to the PPC-05 and the PPC-40 which are two plane-parallel ICs from IBA Dosimetry exhibiting a completely different body material as well as a large difference of cavity size. Each case was investigated in two steps. First, the body material of the reference geometry was modified to match that of the real IC. More specifically, a geometry with a body made of PMMA (PPC-40) and another one with a body made of C552 (PPC-05) were considered. In both cases, the sensitivity of the k_Q factors was studied when geometric tolerances were applied on the entrance window thickness. Then, a second modification was applied, where each geometry has the cavity size corresponding to the sensitive volume of its real IC homologue; i.e. 2 mm of height and 8 mm of radius for the PMMA chamber, and 0.6 mm of height and 5 mm of radius for the C552 chamber. This time the sensitivity of the k_Q was studied when the cavity-related perturbations were applied.

For clarity, these geometries will be referred to as *PPC40-like* and *PPC05-like* in the rest of the manuscript.

Table 2. Summary of the material properties considered in this work. Each material has its corresponding mass density (ρ), WER and ionization potential (I). The WER values were determined via MC simulations (see section 2.4) and the I values were taken from ICRU 90 (Seltzer *et al* 2016).

Material	ρ (g cm^{-3})	WER	I (eV)
Air	0.0012	—	85.7
C552	1.76	1.56	86.8
Graphite	0.93[a]	0.83	81.0
PEEK	1.31	1.25	74.1
PMMA	1.19	1.17	74.0
Water	0.9982	1	78.0

[a] This material refers to a sprayed or painted graphite electrode for which the density must be distinguished from typical graphite densities between 1.8 and 2.1 g cm^{-3}.

2.3. Reference conditions

For the photon simulations, the photon emission spectrum of ^{60}Co described by Mora *et al* (1999) was used, from which a diverging point source positioned 95 cm away from a 20 × 20 × 20 cm^3 water phantom was shaping a 9.5 × 9.5 cm^2 field at its surface.

For the proton simulations, seven mono-energetic proton beams (60, 70, 80, 100, 150, 200 and 250 MeV) and a spread-out Bragg Peak (SOBP) with a range of 15 cm and a modulation of 10 cm were investigated. The latter was taken from Gomà and Sterpin (2019) where the authors superimposed multiple quasi mono-energetic proton beams with different weights. All beams were defined from a uniform 10 × 10 cm^2 field with primary protons having their initial momentum perpendicular to the field. The latter was positioned on the surface of a 20 × 20 × 20 cm^3 water phantom for the SOBP while a 20 × 20 × 5 cm^3 water phantom was considered for the mono-energetic proton beams. This shallower phantom was considered in order to reduce the computational time while maintaining accurate results, since proton backscattering can be neglected (Gomà *et al* 2016).

For photon simulations, a reference depth z_{ref} of 5 g cm^{-2} (where the photon field is a 10 × 10 cm^2) was considered, whereas for proton simulations a reference depth of 1 g cm^{-2} for mono-energetic beams between 60 and 70 MeV, 2 g cm^{-2} for mono-energetic beams between 80 and 250 MeV, and 10 g cm^{-2} (in the middle of the SOBP) for the modulated beam was chosen. These conditions are consistent with the recommendations of the IAEA TRS-398 CoP.

The mean absorbed dose to air ($\bar{D}_{\text{air}}$) was calculated within the air cavity of the ICs, with the centre of the inner surface of the entrance window positioned at z_{ref}. The absorbed dose to water (D_w) on the other hand was calculated inside a cylindrical volume of water having a radius of 1 cm and a height of 250 μm, centred at z_{ref}. With such dimensions, D_w was assumed to be volume independent and thus equivalent to the local dose deposition (Sempau *et al* 2004).

2.4. Water Equivalent Thickness (WET)

In each proton simulation, the positioning of the perturbed IC was corrected for the corresponding WET of the entrance window. As the latter was modified throughout this work, it is more convenient in the following to consider the water equivalent ratio (WER) instead, which is a unitless quantity corresponding to the ratio between the material thickness and its WET (Newhauser and Zhang 2015). The WER of a material has been determined as

$$\text{WER}_{\text{mat.}} = \frac{Z_{\text{d80,water}}}{Z_{\text{d80,mat.}}} \quad , \tag{2}$$

where Z_{d80} denotes the most distal physical depth (expressed in cm) at which the absorbed dose corresponds to 80% of the absorbed dose at the pristine Bragg peak depth. These quantities were derived from depth-dose profiles simulated with the same MC code, and were seen to be rather insensitive to the initial proton beam energy.

All material properties used in this work are presented in table 2.

2.5. Simulation setup

We used GATE (Geant4 Application for Tomographic Emission) version 9.2 (Jan *et al* 2004, Sarrut *et al* 2014), an advanced open source software dedicated to numerical simulations in medical imaging and radiotherapy. The software is based on the MC code Geant4 (GEometry ANd Tracking) version 11.0.0 (Agostinelli *et al* 2003).

The electromagnetic physics was controlled by the physics list *emstandard_opt3* for photon simulations and by *emstandard_opt4* for proton simulations, both of which have been shown to be suited for the

calculation of f_{Q_0} and f_Q factors respectively (Baumann *et al* 2019). In addition, the physics list *QGSP_BIC_HP* which implements hadronic and nuclear processes was used for proton simulations.

In Geant4, a smooth two parameters step function allows to control the step size of a charged particle. The first parameter *(dRoverR)* limits the step size according to the residual range of the particle. As the particle travels, its maximum step size decreases until the range becomes lower than a certain limit defined by the second parameter *(finalRange)* below which the particle is ranged out in a single step. For proton simulations, *dRoverR* was set to 0.05 (Wulff *et al* 2018) and *finalRange* to 100 nm (Baumann *et al* 2020); while for photon simulations, the step size of secondary electrons was controlled by setting *dRoverR* and *finalRange* to 0.003 and 1 nm respectively (O'Brien *et al* 2016).

The minimum range for a new secondary particle to be tracked is determined by a production threshold below which all the energy is deposited locally. To optimise computational time while maintaining accuracy, a cut of 500 μm was applied in the water phantom which was reduced to 1 μm inside the IC geometry. In addition, to avoid any perturbation in the secondary particle fluence due to the cut gradient between two regions, an envelope of 600 μm was defined around the IC, within which the production cut was also set to 1 μm. The thickness of the envelope corresponds to the external production cut times a safety factor of 1.2 allowing to account for range straggling (Sempau and Andreo 2006).

In this study, the simulations were chosen to run until the MC reached a certain statistical precision, expressed below as the standard deviation σ. This allowed to have homogeneous error bars across the different beam energies considered (at the cost of longer running times for high energy proton beam simulations). For dose to water simulations the statistical precision was set to about 0.05% for protons and about 0.1% for photons, while dose to air simulations were achieved with a statistical precision of about 0.1% for protons and about 0.3%–0.4% for photons. Therefore, a type-A uncertainty of about 0.7% is associated to all the k_Q factors calculated in this work. It should be noted that these uncertainties correspond to the typical magnitude of the uncertainties that can be found in MC calculated k_Q publications (see for example Andreo *et al* 2020 for f_{Q_0} uncertainties and Baumann *et al* 2023 for f_Q and k_Q uncertainties).

3. Results

In this section, all the results are presented as the relative deviations between perturbed and reference geometries. The agreement between the data is then quantified according to the combined type-A uncertainty of the compared results.

3.1. General impact of tolerances

The results for the f_{Q_0} factors are depicted in figure 2. The relative deviations are presented both for single perturbations and for a combination of multiple perturbations. In the latter case, the combination of linear tolerances including the perturbation of the entrance window, of the cavity height and of the exit window, is distinguished from the radial tolerances including the cavity radius and the lateral thickness of the body. In both situations, all the parameters were set simultaneously either to their upper or lower values. All the results show an agreement at the 1σ level (within 0.5%) with the reference geometry, with the largest deviation being of the order of 0.4%.

The same results for the f_Q factors are presented in figure 3, with the radial perturbations plotted in the upper panel of the figure and the linear perturbations plotted in the lower panel, for the eight different beam qualities. All the results show an agreement at the 2σ level (within 0.4%) with the largest deviation observed being of the order of 0.3%. No clear trend or energy dependence could be highlighted.

Finally, the results derived for the k_Q factors (calculated from equation (1)) are presented in the top and middle panels of figure 4. All the results show an agreement at the 1σ level (within 0.55%) with the reference geometry, and largest deviation observed is of about 0.5%.

3.2. Impact of tolerances for modified geometries

The results for the PPC-like ICs and for the geometries with graphite electrodes are presented in this subsection. In all cases, similar results were obtained for the *f* factors, with an agreement at the 1σ level for photons (f_{Q_0}) and an agreement at the 2σ level for protons (f_Q).

The results obtained for the k_Q factors of the PPC40-like and of the PPC05-like ICs when the perturbation is applied to their entrance window are shown in the lower panel of figure 4. The results for the perturbed geometries show an agreement at the 1σ level with their respective reference geometries, with a deviation of less than 0.5%. The same figure depicts the results obtained for the PPC-like ICs modelled with the air cavity size of their homologous IC, and perturbed as described above. The results do not show any significant sensitivity from cavity-related combined tolerances, as an agreement is observed at the 1σ level.

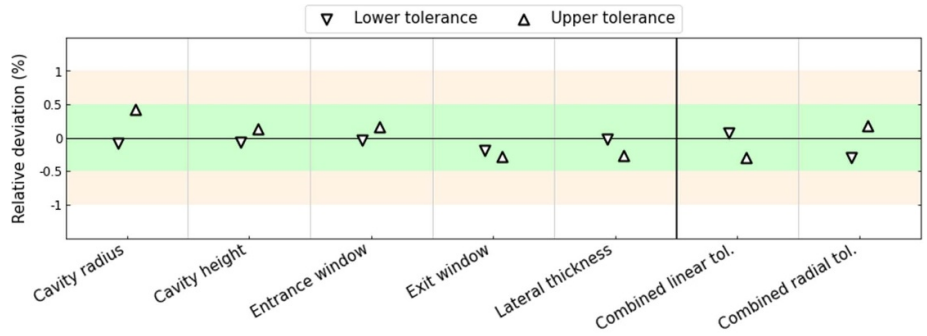

Figure 2. Relative deviation of f_{Q_0} factors compared to the reference geometry. Combining the type-A uncertainty on the reference geometry and on the perturbed geometry, an agreement at the 1σ level is achieved within the green region while an agreement at the 2σ level is achieved within the orange region. The vertical black line was added for visualisation purposes to distinguish single-parameter perturbations to combined-parameter perturbations.

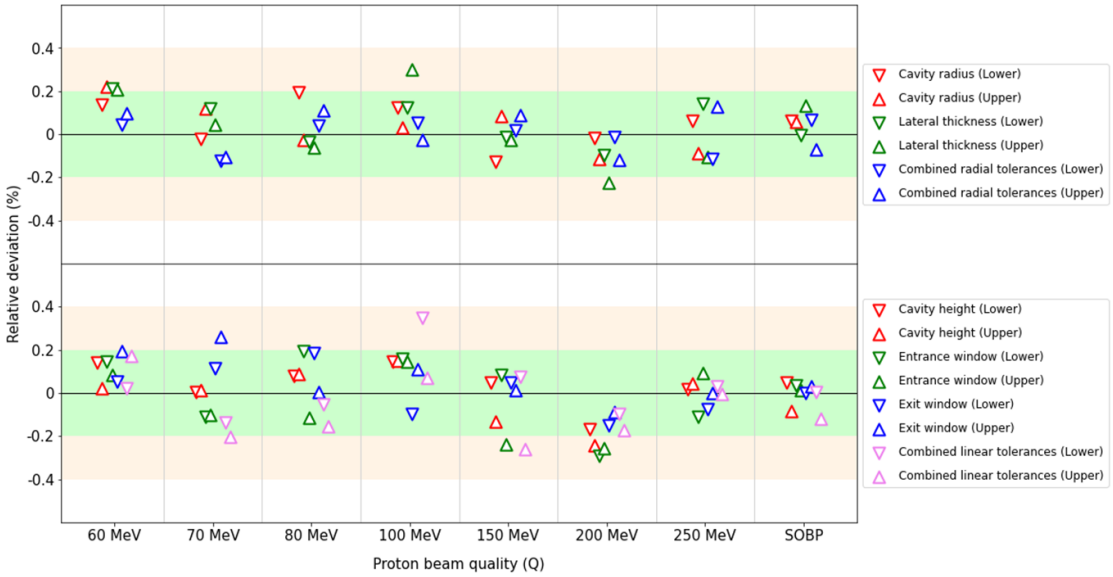

Figure 3. Relative deviation of f_Q factors compared to the reference geometry. Combining the type-A uncertainty on the reference geometry and on the perturbed geometry, an agreement at the 1σ level is achieved within the green region while an agreement at the 2σ level is achieved within the orange region. The results are presented for mono-energetic proton beams with energies between 60 and 250 MeV, as well as for one SOBP. The upper panel depicts radial perturbations while the lower panel depicts linear perturbations.

Finally, the results of the k_Q factors after a perturbation of the electrode thickness are depicted in figure 5. An agreement at the 1σ was observed for both the top electrode and for the collecting electrode, with deviations not exceeding 0.5%.

4. Discussion

4.1. Application of general tolerances

Using MC calculation, we showed that the beam quality correction factor is not sensitive to manufacturing tolerances of about 10% that one can typically find on plane-parallel ICs. By these words, we mean that any deviation observed remained within the significance of calculation uncertainty, corresponding to an agreement at the 1σ level from reference conditions.

Overall, photon results were seen to be the largest source of deviations compared to proton results. This behaviour is simply due to the difference of statistical precision aimed on both types of simulations. For each case study i.e. all k_Q values determined for a given geometry throughout the proton energy spectrum considered; we used an unique value of the f_{Q_0} factor. This is a common procedure in the current determination of k_Q factors using MC (see e.g. Gomà and Sterpin 2019, Baumann *et al* 2019), but it means that any statistical fluctuation coming from photon simulations will be propagated on every k_Q values, introducing an intrinsic source of correlation between the k_Q factors. This correlation can be seen by the shift

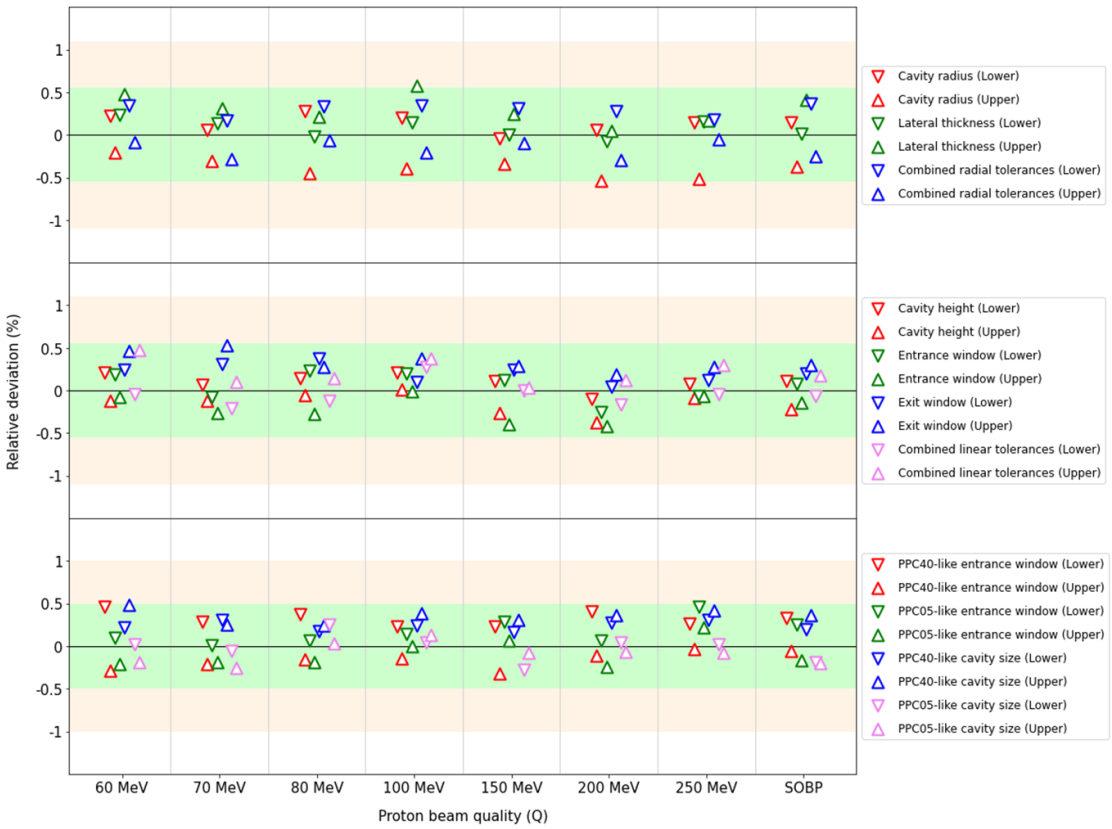

Figure 4. Relative deviation of k_Q factors compared to the reference geometry. Combining the type-A uncertainty on the reference geometry and on the perturbed geometry, an agreement at the 1σ level is achieved within the green region while an agreement at the 2σ level is achieved within the orange region. The results are presented for mono-energetic proton beams with energies between 60 and 250 MeV, as well as for one SOBP. Radial perturbations are depicted in the upper panel, linear perturbations in the middle panel, and the results for PPC-like geometries are depicted in the lower panel.

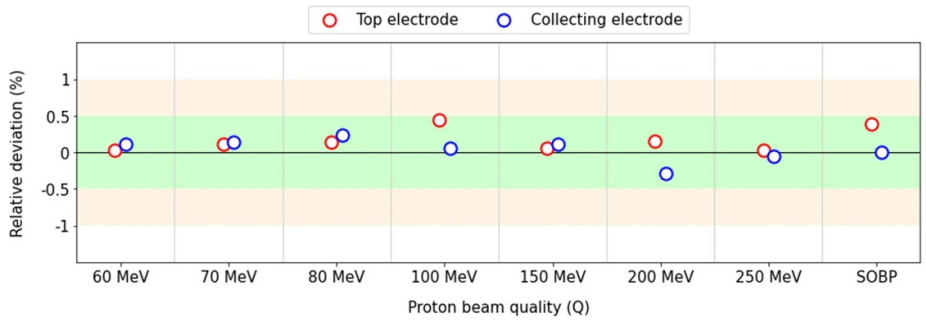

Figure 5. Relative deviation of k_Q factors for the top electrode (red) and for the collecting electrode (blue) with a thickness of 0.1 mm compared to their respective reference geometry with an electrode thickness of 0.05 mm. Combining the type-A uncertainty on the reference geometry and on the perturbed geometry, an agreement at the 1σ level is achieved within the green region while an agreement at the 2σ level is achieved within the orange region. The results are presented for mono-energetic proton beams with energies between 60 and 250 MeV, as well as for one SOBP.

of the k_Q values compared to the results of the f_Q factors for the same scenario. A visual example of this behaviour can be observed in the results depicted for upper tolerances applied on the radius of the air cavity. In the upper panel of figure 3, we can first see that the deviations of the f_Q factors lie between -0.1% and 0.2% for all proton beam energies considered. Then, given that the deviation of the f_{Q_0} in figure 2 is about 0.4%, the final deviations of the k_Q factors $(\propto f_Q/f_{Q_0})$ are therefore logically between -0.5% and -0.2%.

As the statistical uncertainty established on the k_Q factors in this study (about 0.7%) is of the same order of magnitude as the uncertainty of the MC calculated k_Q values used in the TRS-398 CoP (between 0.7% and 1.2%); our results suggest that any fluctuation arising from geometric tolerances must be significantly smaller than the overall statistical uncertainty and that this sensitivity of the k_Q factors cannot be observed

with the current precision. This statement can be made for all proton beam energies considered, between 60 MeV and 250 MeV as well as for the investigated SOBP.

4.2. Impact of the entrance window

From the results presented in figure 4, we observed that the perturbations of the entrance window did not significantly impact the k_Q values, no matter the material considered for the chamber body. In each scenario, the positioning of the chamber was corrected according to the WET of the entrance window meaning that as long as the chamber is correctly positioned, small deviations in the entrance window thickness are not expected to lead to significant deviations of the k_Q values. However, in practice, during reference dosimetry measurements, these conditions are not always achieved. Indeed, users typically rely on the nominal thickness of the entrance window to apply the WET correction. For example, considering the WER of PEEK, PMMA and C552, a difference of 10% in the entrance window thickness would lead to a mispositioning of the chamber between 0.12 mm and 0.13 mm for PMMA and PEEK, and of about 0.16 mm for C552. We studied this effect for each of the three materials by applying the same perturbations to the entrance window (as described above), but this time only considering the nominal WET from the reference geometry. In all cases, we found that even in these conditions, the values of the k_Q factors remain in agreement at the 1σ level with the reference geometry. Hence, such perturbation should not be significant for all ICs having their entrance window made of a material having a density lighter than C552. In the case of heavier materials, the main concern is expected to be at low energy where the dose gradient is higher at z_{ref} for mono-energetic proton beams.

4.3. PPC-like chambers

In the previous section, we showed that our model of PPC05-like and PPC40-like ICs do not show k_Q sensitivity to entrance window perturbations within calculated uncertainties. To get closer to the real plane-parallel IC geometries, we adapted the size of each air cavity as described in section 2.2.2. The results presented in the lower panel of figure 4 show that in both cases the k_Q factor does not significantly change under air cavity perturbations, although there is a factor 8 between the cavity volumes of the two geometries studied.

Obviously, real plane-parallel IC do not have such simple geometries. In real cases, the chambers are made of more than 20 different components that can be made of different materials with various elemental compositions and various densities. However, under proton beams, as the backscattering is negligible, we assumed that the most problematic part of the chambers would be those being between the particle source and the air cavity. Hence, as no sensitivity was observed from the entrance window, from the graphite electrode nor from the air cavity itself, and this for various geometries; we can state that manufacturing tolerances studied in this work do not represent a concern for the current k_Q factors applied on plane-parallel ICs. Note that the modelling of the guard region was not considered relevant here as no electric field was introduced within the air cavity.

4.4. Estimated contribution to MC results

Considering the statistical uncertainties on the MC calculated quantities in this study (see section 2.5), the total uncertainty budget on the k_Q values coming from the MC part (i.e. f_Q/f_{Q_0}) was about 0.4%. Taking into account the largest deviation of the perturbed k_Q factors observed from figure 4 (which is about 0.55% to be conservative), we can estimate an upper limit on the added uncertainty due to manufacturing tolerances on MC calculated k_Q factors to be about 0.7%. Of course, this contribution should be confirmed in future works for real chamber geometries in combination with an improvement of the statistics.

4.5. Comment on cylindrical chambers

In this section, we briefly discuss how our results could be extended to cylindrical IC geometries. To do this, we divide a cylindrical IC into four regions, namely the shell, the air cavity, the central electrode and the back of the IC (stem + sleeve).

The air cavity of cylindrical and plane-parallel ICs is quite similar (the difference being the beam incidence on the curved surface of the cylinder), small deviations in the cavity dimension are therefore not expected to influence the averaged deposited dose.

Regarding the back of the chamber, (Baumann *et al* 2021) showed that the perturbation factors for stem and sleeve (p_{stem} and p_{sleeve} respectively) were generally within 0.5% of unity for the various cylindrical ICs that the authors considered. Therefore, the influence of the back of a cylindrical IC on the k_Q factors is negligible and can be expected to remain so even for small dimensional deviations from manufacturing tolerance (about 10% of the radius).

In the case of entrance window, cylindrical ICs contain a shell with constant thickness all around their collecting volume. Considering the thickness of the shell at the top of the IC lying on the z-axis, the beam will see the shell thickness increase as we move away from the z-axis due to the curvature of the chamber. Therefore, considering a 10% increase of the shell thickness, the particle beam will actually cross a thicker layer (which can reach 20% for some ICs) depending on the position where the particles enter the shell/cavity. This is in contrast to plane-parallel ICs where the thickness remains constant for all entry points in the entrance window. Further investigation is required to understand if this feature can affect the k_Q values.

Finally, considering the central electrode of cylindrical ICs, no parallel can be made with plane-parallel ICs, which therefore definitely requires additional investigation.

5. Conclusion

The sensitivity of the MC calculated k_Q factors was studied for geometric perturbations coming from typical manufacturing tolerances of about 10% applied on plane-parallel ICs. Considering a representative model of plane-parallel IC, we showed that none of the tolerances coming from entrance and exit windows, air cavity size nor from the lateral thickness of the casing could significantly impact the k_Q values given the current type-A uncertainty associated to k_Q factors i.e. 0.7%. We also showed that this impact remains insignificant when considering more realistic geometries either in PMMA or in C552, or when adding graphite electrodes. Finally, within the framework of our study, we could estimate the maximum added uncertainty from manufacturing tolerances applied to MC calculated k_Q values to be 0.7%.

Finally, as no significant influence was observed, the current use of nominal ICs dimensions obtained from manufacturers blueprints remains consistent for the modelling of plane-parallel ICs used in the MC calculation of k_Q factors; which supports the last results recommended by the TRS-398 CoP.

Data availability statement

All data that support the findings of this study are included within the article (and any supplementary information files).

Acknowledgments

Computational resources have been provided by the Consortium des Équipements de Calcul Intensif (CÉCI), funded by the Fonds de la Recherche Scientifique de Belgique (F.R.S.-FNRS) under Grant No. 2.5020.11 and by the Walloon Region.

Guillaume Houyoux is funded by the Walloon Region, MecaTech and BioWin Clusters (D-CAF Project, No 8510).

We would like to thank IBA Dosimetry for sharing with us IC blueprints, and also Kilian-Simon Baumann for valuable discussions.

ORCID iDs

Guillaume Houyoux https://orcid.org/0009-0008-8825-1520
Sébastien Penninckx https://orcid.org/0000-0002-3016-778X
Séverine Rossomme https://orcid.org/0000-0001-8560-7642
Kevin Souris https://orcid.org/0000-0003-4124-6149
Hugo Palmans https://orcid.org/0000-0002-0235-5118
Nick Reynaert https://orcid.org/0000-0001-9221-9103

References

Agostinelli S *et al* 2003 Geant4-a simulation toolkit *Nucl. Instrum. Methods Phys. Res.* A **506** 250–303

Andreo P *et al* 2020 Determination of consensus kq values for megavoltage photon beams for the update of iaea trs-398 *Phys. Med. Biol.* **65** 095011

Andreo P, Wulff J, Burns D T and Palmans H 2013 Consistency in reference radiotherapy dosimetry: resolution of an apparent conundrum when 60co is the reference quality for charged-particle and photon beams *Phys. Med. Biol.* **58** 6593

Baumann K-S, Gomà C, Wulff J, Kretschmer J and Zink K 2023 Monte carlo calculated ionization chamber correction factors in clinical proton beams–deriving uncertainties from published data *Phys. Med.* **113** 102655

Baumann K-S, Horst F, Zink K and Gomà C 2019 Comparison of penh, fluka and geant4/topas for absorbed dose calculations in air cavities representing ionization chambers in high-energy photon and proton beams *Med. Phys.* **46** 4639–53

Baumann K-S, Kaupa S, Bach C, Engenhart-Cabillic R and Zink K 2020 Monte carlo calculation of beam quality correction factors in proton beams using topas/geant4 *Phys. Med. Biol.* **65** 055015

Baumann K-S, Kaupa S, Bach C, Engenhart-Cabillic R and Zink K 2021 Monte carlo calculation of perturbation correction factors for air-filled ionization chambers in clinical proton beams using topas/geant *Z. Med. Phys.* **31** 175–91
Gomà C, Andreo P and Sempau J 2016 Monte carlo calculation of beam quality correction factors in proton beams using detailed simulation of ionization chambers *Phys. Med. Biol.* **61** 2389
Gomà C and Sterpin E 2019 Monte carlo calculation of beam quality correction factors in proton beams using penh *Phys. Med. Biol.* **64** 185009
IAEA 2024 Absorbed dose determination in external beam radiotherapy. No. 398 (Rev. 1) *Technical Reports Series* (International Atomic Energy Agency)
ISO 2768-1 1989 General tolerances—Part 1: tolerances for linear and angular dimensions without individual tolerance indications *Technical Report* (International Organization for Standardization)
Jan S *et al* 2004 Gate: a simulation toolkit for pet and spect *Phys. Med. Biol.* **49** 4543
Kurtz S M 2012 Chemical and radiation stability of peek *Peek Biomaterials Handbook* (Elsevier) pp 75–79
McNiven A L, Umoh J, Kron T, Holdsworth D W and Battista J J 2008 Ionization chamber volume determination and quality assurance using micro-ct imaging *Phys. Med. Biol.* **53** 5029
Mora G, Maio A and Rogers D 1999 Monte carlo simulation of a typical therapy source *Med. Phys.* **26** 2494–502
Muir B, McEwen M and Rogers D 2012 Beam quality conversion factors for parallel-plate ionization chambers in mv photon beams *Med. Phys.* **39** 1618–31
Muir B and Rogers D 2010 Monte carlo calculations of, the beam quality conversion factor *Med. Phys.* **37** 5939–50
Muir B and Rogers D 2013 Monte carlo calculations for reference dosimetry of electron beams with the ptw roos and ne2571 ion chambers *Med. Phys.* **40** 121722
Newhauser W D and Zhang R 2015 The physics of proton therapy *Phys. Med. Biol.* **60** R155
O'Brien D, Roberts D, Ibbott G and Sawakuchi G 2016 Reference dosimetry in magnetic fields: formalism and ionization chamber correction factors *Med. Phys.* **43** 4915–27
Palmans H, Lourenço A, Medin J, Vatnitsky S and Andreo P 2022 Current best estimates of beam quality correction factors for reference dosimetry of clinical proton beams *Phys. Med. Biol.* **67** 195012
Perl J, Shin J, Schümann J, Faddegon B and Paganetti H 2012 Topas: an innovative proton monte carlo platform for research and clinical applications *Med. Phys.* **39** 6818–37
Sarrut D *et al* 2014 A review of the use and potential of the gate monte carlo simulation code for radiation therapy and dosimetry applications *Med. Phys.* **41** 064301
Seltzer S, Fernandez-Varea J, Andreo P, Bergstrom P, Burns D, Krajcar Bronić I, Ross C and Salvat F 2016 Key data for ionizing-radiation dosimetry: measurement standards and applications *ICRU Report* 90
Sempau J and Andreo P 2006 Configuration of the electron transport algorithm of penelope to simulate ion chambers *Phys. Med. Biol.* **51** 3533
Sempau J, Andreo P, Aldana J, Mazurier J and Salvat F 2004 Electron beam quality correction factors for plane-parallel ionization chambers: Monte carlo calculations using the penelope system *Phys. Med. Biol.* **49** 4427
Wulff J, Baumann K-S, Verbeek N, Bäumer C, Timmermann B and Zink K 2018 Topas/geant4 configuration for ionization chamber calculations in proton beams *Phys. Med. Biol.* **63** 115013
Wulff J, Heverhagen J, Zink K and Kawrakow I 2010 Investigation of systematic uncertainties in monte carlo-calculated beam quality correction factors *Phys. Med. Biol.* **55** 4481
Zink K and Wulff J 2012 Beam quality corrections for parallel-plate ion chambers in electron reference dosimetry *Phys. Med. Biol.* **57** 1831